Tuning Organogels and Mesophases with Phenanthroline Ligands and Their Copper Complexes by Inter- to Intramolecular Hydrogen Bonds

Raymond Ziessel,*,[†] Guillaume Pickaert,[†] Franck Camerel,[†] Bertrand Donnio,[||] Daniel Guillon,[||] Michèle Cesario,[‡] and Thierry Prangé[§]

Contribution from the Laboratoire de Chimie Moléculaire, Université Louis Pasteur, Ecole Chimie, Polymères, Matériaux (ECPM), Centre National de la Recherche Scientifique (CNRS), 25 rue Becquerel, F-67008 Strasbourg Cedex, France, Institut de Physique et Chimie des Matériaux de Strasbourg (IPCMS), Groupe de Matériaux Organiques (GMO), Université Louis Pasteur-CNRS (UMR 7504), 23 rue du Loess, BP 43, F-67034 Strasbourg Cedex 2, France, Institut de Chimie des Substances Naturelles, CNRS, F-91128 Gif-sur-Yvette, France, LURE, Bât. 209d, Université Paris-Sud, BP 34, F-91898 Orsay Cedex, France, and LCRB, Faculté de Pharmacie, 4 Av de l'Observatoire, F-75006 Paris, France

Received May 18, 2004; E-mail: ziessel@chimie.u-strasbg.fr

Abstract: A novel family of highly functionalized molecules consisting of a central 4-methyl-3,5-diacylaminobenzene platform linked in close proximity to the methyl group by two lateral aromatic rings each equipped with two long alkoxy chains has been rationally designed. The presence of amide tethers and a chelating phenanthroline fragment connected via an ester dipole formed a new class of gelating reagents and mesomorphic materials. A few of these compounds have the tendency to form macromolecule-like aggregates through noncovalent interactions in hydrocarbon solvents and were found to exhibit thermotropic cubic mesophases. In light of the X-ray molecular structure of the methoxy ligand, an infinite network maintained by intermolecular hydrogen bonds as well as by $\pi-\pi$ stacking of the phenyl subunits was evidenced. FT-IR studies confirm that the common driving force for aggregation in the organogels and microsegregation in the mesophase is the occurrence of a tight intermolecular H-bonded network that does not persist in diluted solution. This situation is switched when the ligands are interlocked by a copper-(I) cation. A strong intramolecular H-bond confirmed by X-ray diffraction of a single crystal for the methoxy case provides very stable complexes but inhibits the gelation of the solvents. Heating the complexes bearing long paraffin chains ($n = 12$ and 16) in the dried state leads to a self-organization into a columnar liquid-crystalline phase in which the columns are arranged along a 2D oblique symmetry as deduced from powder XRD experiments. In this case, the complexes with the appended counteranions self-assemble in a specific way to form columns. A striking observation is that the intramolecular hydrogen bond persists in the mesophase as it does in solution without any evidence of an extended network. As far as we are aware, these ligands and complexes are rare examples in which organogelation and thermotropic mesomorphic behavior could be observed in parallel with molecules bearing a chelating platform. Due to the synthetic availability of the 4-methyl-3,5-diacylaminobenzene core and the simplicity by which the chelating platforms can be graphed, this methodology represents a practical alternative to the production of functionalized organogelators and mesomorphic materials.

Introduction

Intermolecular hydrogen bonding is a very topical area of study because of its relevance to a variety of naturally occurring processes, such as recognition and assembly of complementary nucleobases that stabilize the double helical structure of nucleic acids, but also in hydrogels of biopolymers for biomedical applications.[1] The ability to manipulate, switch, or frustrate H-bonded arrays also opens novel perspectives for materials

science. The tailoring and design of such materials with multiple functions is a subject of intense research that holds promise for the rational design of nanostructures with well-defined channels and physical properties.[2] Along these lines, intermolecular hydrogen bonding has been employed for the engineering of

[†] LCM, ECPM, ULP.
[‡] Institut de Chimie des Substances Naturelles.
[§] Université Paris-Sud & Faculté de Pharmacie.
[||] IPCMS, GMO.

(1) Uhrich, K. E.; Cannizzaro, S. M.; Langer, R. S.; Shakesheff, K. M. *Chem. Rev.* **1999**, *99*, 3181.
(2) (a) Muthukumar, M.; Ober, C. K.; Ober, E. L.; Thomas, E. L. *Science* **1997**, *277*, 1225. (b) Stupp, S. I.; Braun, P. V. *Science* **1997**, *277*, 1242. (c) Chen, Z.-R.; Kornfield, J. A.; Smith, S. S.; Grothaus, J. T.; Satkowski, M. M. *Science* **1997**, *277*, 1248. (d) Smith, R. C.; Fischer, W. M.; Gin, D. L. *J. Am. Chem. Soc.* **1997**, *119*, 4092. (e) Deng, H.; Gin, D. L.; Smith, R. C. *J. Am. Chem. Soc.* **1997**, *119*, 4092. (f) Miller, A.; Kim, E.; Gray, D. H.; Gin, D. L. *Angew. Chem., Int. Ed.* **1999**, *38*, 3022.

organic liquid crystals, (organo)gelators, well-defined nanometer-scale or mesoscopic assemblies, thin films, and polymeric materials that self-assemble from simple elementary units.[3-5] It is well accepted that hierarchical self-organization events involving hydrogen bonding are of significant importance to the formation of liquid-crystalline phases but also for the stabilization of existing mesophases.[6,7] However, H-bonded metallomesogens[8] have been scarcely described despite the realization that they might possess unusual properties.[9]

Hydrogen bonds are commonly responsible for solvent immobilization by organogelators and to a lesser extent for water gelation by hydrogelators.[5,10] In both cases, to achieve gelation, there must be a balance between the tendency of the molecules to dissolve or to aggregate. The same feature is true for achieving a mesomorphic state for which a balance is required between the tendency of the molecules to melt or to microsegregate into a noncrystalline state. Likewise, it is more difficult to find low molecular compounds capable of gelling solvents and exhibiting a thermotropic mesomorphic behavior.[11-13]

Molecular recognition and self-assembling processes directed by complementary hydrogen bonding have received attention for controlling molecular structures.[14-16] In general, hydrogen bonding in artificial molecular systems is most effective in solid states or in noncompetitive aprotic organic solvents. However, recent findings demonstrate that molecular recognition via hydrogen bonding was also effective at the air–water interface, in bulk water, or in the lyotropic liquid-crystalline state.[17,18]

In some studies, pyridyl or bipyridyl moieties have been used as basic building blocks for the construction of mesomorphic frameworks[19,20] and also as hydrogen-bond acceptors.[21,22] In most of these examples, the engineering of liquid-crystalline ligands is feasible but when complexed with transition metals, the mesomorphic property is lost due to the introduction of additional dipoles, geometric demands of the metal, charges, and bulkiness of the metal center and surrounding ligands. However, in other cases, nonmesomorphic ligands allowed one to prepare metallomesogens by wrapping the ligands around metals.[23,24] The shape of the molecule and the balance between the rigid core and the paraffin chains must sustain microsegregation during the heating cycle. In some rare cases, both ligands and complexes display mesomorphism.[25,26] One way to overcome these difficulties is to engineer a system in which additional supramolecular binding directors (such as hydrogen bonding) would stabilize the mesophase in both cases (ligand and complex). It is surmised that these additional vectors would stabilize the mesophase within the ligand via intermolecular hydrogen bonding, whereas in the case of the complex this hydrogen bonding is switched into intramolecular bonds stabilizing the interlocked molecular structure. Extension of the concept of directional intermolecular interactions to organogels would allow the gelation or nongelation of specific solvents. Such a system is the aim of the present contribution, where we use derivatized phenanthroline (phen) cores equipped with amide linkage to generate cationic copper(I) and mesogenic materials. The switching from inter- to intrahydrogen bonding is highlighted by the reversible immobilization of the solvent by the ligands but not by the complexes.

As a matter of fact, mesomorphic (lyotropic or thermotropic)-derivatized phenanthroline chelates are rare and are never involved in hydrogen-bonded networks.[27,28] More surprisingly, only a few references describe thermotropic metal-containing

(3) (a) Hirschberg, J. H. K. K.; Brunsveld, L.; Ramzi, A.; Vekemans, J. A. J. M.; Sibesma, R. P.; Meijer, E. W. *Nature* **2000**, *407*, 167. (b) Jonkheijm, P.; Miura, A.; Zdanowska, M.; Hoeben, F. J. M.; De Feyter, S.; Schenning, A. P. H. J.; De Schryver, F. C.; Meijer, E. W. *Angew. Chem., Int. Ed.* **2004**, *4*, 74.

(4) (a) Paleos, C. M.; Tsiourvas, D. *Angew. Chem., Int. Ed. Engl.* **1995**, *34*, 1696. (b) Tschierske, C. *Prog. Polym. Sci.* **1996**, *21*, 775. (c) Kato, T. *Struct. Bonding* **2000**, *96*, 95. (d) Lee, H. K.; Lee, H.; Ko, Y. H.; Chang, Y. J.; Oh, N.-K.; Zin, W.-C.; Kim, K. *Angew. Chem., Int. Ed.* **2001**, *40*, 2669. (e) Paleos, C. M.; Tsiourvas, D. *Liq. Cryst.* **2001**, *28*, 1127. (f) Yoshikawa, I.; Li, J.; Sakata, Y.; Araki, K. *Angew. Chem., Int. Ed.* **2004**, *43*, 100.

(5) Terech, P.; Weiss, R. G. *Chem. Rev.* **1997**, *97*, 3133.

(6) (a) Brienne, M.-J.; Gabard, J.; Lehn, J.-M.; Stibor, I. *J. Chem. Soc., Chem. Commun.* **1989**, 1868. (b) Fouquey, C.; Lehn, J.-M.; Levelut, A.-M. *Adv. Mater.* **1990**, *2*, 254. (c) Antonietti, M.; Heinz, S. *Nachr. Chem. Technol. Lab.* **1992**, *40*, 308. (d) Lehn, J.-M. *Makromol. Chem., Macromol. Symp.* **1993**, *69*, 1. (e) Gulik-Krzywicki, T.; Fouquey, C.; Lehn, J.-M. *Proc. Natl. Acad. Sci. U.S.A.* **1993**, *90*, 163. (f) Kotera, M.; Lehn, J.-M.; Vigneron, J.-P. *J. Chem. Soc., Chem. Commun.* **1994**, 197. (g) Marchi-Artzner, V.; Jullien, L.; Gulik-Krzywicki, T.; Lehn, J.-M. *Chem. Commun.* **1997**, 117.

(7) (a) Matsunaga, Y.; Terada, M. *Mol. Cryst. Liq. Cryst.* **1986**, *141*, 321. (b) Kawada, H.; Matsunaga, Y.; Takamura, T.; Terada, M. *Can. J. Chem.* **1988**, *66*, 1867. (c) Praefcke, K.; Levelut, A.-M.; Kohne, B.; Eckert, A. *Liq. Cryst.* **1989**, *6*, 263. (d) Ebert, M.; Kleppinger, R.; Soliman, M.; Wolf, M.; Wendorf, J. H.; Latterman, G.; Staufer, G. *Liq. Cryst.* **1990**, *7*, 553. (e) Tomazos, D.; Out, G.; Heck, J. A.; Johansson, G.; Percec, V.; Môller, M. *Mol. Cryst. Liq. Cryst.* **1991**, *16*, 509. (f) Festag, R.; Kleppinger, R.; Soliman, M.; Wendorff, J. H.; Latterman, G.; Staufer, G. *Liq. Cryst.* **1992**, *11*, 699. (g) Malthête, J.; Levelut, A.-M.; Liébert, L. *Adv. Mater.* **1992**, *4*, 37. (h) Kato, T.; Kihara, H.; Kumar, U.; Uryu, T.; Fréchet, J. M. *Angew. Chem., Int. Ed. Engl.* **1994**, *33*, 1644. (i) Malthête, J.; Davidson, P. *Bull. Soc. Chim. Fr.* **1994**, *131*, 812. (j) Kleppinger, R.; Lillya, C. P.; Yang, C. *Angew. Chem., Int. Ed. Engl.* **1995**, *34*, 1637. (k) Albouy, P. A.; Guillon, D.; Heinrich, B.; Levelut, A.-M.; Malthête, J. *J. Phys. II Fr.* **1995**, *5*, 1617. (l) Koh, K. N.; Araki, K.; Komori, T.; Shinkai, S. *Tetrahedron Lett.* **1995**, *36*, 5191. (m) Palmans, A. R. A.; Vekemans, J. A. J. M.; Fischer, H.; Hikmet, R. A.; Meijer, E. W. *Chem.-Eur. J.* **1997**, *3*, 300. (n) Kleppinger, R.; Lillya, C. P.; Yang, C. *J. Am. Chem. Soc.* **1997**, *119*, 4097. (o) Kato, T.; Kubota, Y.; Uryu, T.; Ujiie, S. *Angew. Chem., Int. Ed. Engl.* **1997**, *36*, 1617. (p) Suarez, M.; Lehn, J.-M.; Zimmerman, S. C.; Skoulios, A.; Heinrich, H. *J. Am. Chem. Soc.* **1998**, *120*, 9526.

(8) Donnio, B.; Guillon, D.; Bruce, D. W.; Deschenaux, R. Metallomesogens. In *Comprehensive Coordination Chemistry II: From Biology to Nanotechnology*; McCleverty, J. A., Meyer, T. J., Eds.; Elsevier: Oxford, U.K., 2003; Vol. 7, Chapter 7.9 (Fujita, M., Powell, A., Eds.), pp 357–627.

(9) Deschenaux, R.; Monnet, F.; Serrano, E.; Turpin, F.; Levelut, A.-M. *Helv. Chim. Acta* **1998**, *81*, 2072.

(10) Estoff, L. A.; Hamilton, A. D. *Chem. Rev.* **2004**, *104*, 1201.

(11) (a) Ohta, K.; Hasebe, H.; Moriya, M.; Fujimoto, T.; Yamamoto, I. *J. Mater. Chem.* **1991**, *1*, 831. (b) Ohta, K.; Moriya, M.; Ikejima, M.; Hasebe, H.; Kobayashi, N.; Yamamoto, I. *Bull. Chem. Soc. Jpn.* **1997**, *70*, 1199. (c) Van Gorp, J. J.; Vekemans, J. A. J. M.; Meijer, E. W. *J. Am. Chem. Soc.* **2002**, *124*, 14759.

(12) (a) Kato, T. *Struct. Bonding* **2000**, *96*, 95. (b) Mizoshita, N.; Monobe, H.; Inoue, M.; Ukon, M.; Watanabe, T.; Shimizu, Y.; Hanabusa, K.; Kato, T. *Chem. Commun.* **2002**, 428.

(13) Camerel, F.; Faul, C. F. J. *Chem. Commun.* **2003**, 1958.

(14) (a) Rebek, J., Jr. *Acc. Chem. Res.* **1990**, *23*, 99. (b) Garcia-Tellado, F.; Geib, S. J.; Goswami, S.; Hamilton, A. D. *J. Am. Chem. Soc.* **1991**, *113*, 9265.

(15) Lehn, J.-M.; Mascal, M.; Decian, A.; Fischer, J. *J. Chem. Soc., Perkin Trans. 2* **1992**, 461.

(16) (a) Seto, C. T.; Whitesides, G. M. *J. Am. Chem. Soc.* **1990**, *112*, 6409. (b) Zerkowski, J. A.; Seto, C. T.; Whitesides, G. M. *J. Am. Chem. Soc.* **1992**, *114*, 5473.

(17) Sasaki, D. Y.; Kurihara, K.; Kunitake, T. *J. Am. Chem. Soc.* **1991**, *113*, 9685 and references therein.

(18) Kimizuka, N.; Kawasaki, T.; Kunitake, T. *J. Am. Chem. Soc.* **1993**, *115*, 4387.

(19) (a) Bruce, D. W.; Rowe, K. E. *Liq. Cryst.* **1995**, *18*, 161; **1996**, *20*, 183. (b) Bruce, D. W.; Rowe, K. E. *J. Chem. Soc., Dalton Trans.* **1995**, 3913.

(20) (a) El-ghayoury, A.; Douce, L.; Skoulios, A.; Ziessel, R. *Angew. Chem., Int. Ed.* **1998**, *37*, 2205. (b) Douce, L.; El-ghayoury, A.; Skoulios, A.; Ziessel, R. *Chem. Commun.* **1999**, 2033.

(21) (a) Sideratou, Z.; Paleos, C. M.; Skoulios, A. *Mol. Cryst. Liq. Cryst.* **1995**, *265*, 19. (b) Koga, T.; Ohba, H.; Takase, H.; Sakagami, S. *Chem. Lett.* **1994**, 2071.

(22) (a) Palmans, A. R. A.; Vekemans, J. A. J. M.; Fischer, H.; Hikmet, R. A.; Meijer, E. W. *Chem.-Eur. J.* **1997**, *3*, 300. (b) Douce, L.; Ziessel, R.; Lai, H.-H.; Lin, H.-C. *Liq. Cryst.* **1999**, *26*, 1797. (c) Brunveld, L.; Lohmeijer, B. G. G.; Vekmans, J. A. J. M.; Meijer, E. W. *Chem. Commun.* **2000**, 2305.

(23) Ziessel, R. *Coord. Chem. Rev.* **2001**, *216–217*, 195.

(24) Douce, L.; Ziessel, R. *Mol. Cryst. Liq. Cryst.* **2001**, *362*, 133.

(25) Rowe, K.; Bruce, D. W. *Mol. Cryst. Liq. Cryst.* **1999**, *326*, 15.

(26) Okamoto, K.; Matsuoka, Y.; Wakabayashi, Yamagishi, A.; Hoshino, N. *Chem. Commun.* **2002**, 282.

(27) Munoz, S.; Gokel, G. W. *J. Am. Chem. Soc.* **1993**, *115*, 4899.

(28) Bousquet, S. J. P.; Bruce, D. W. *J. Mater. Chem.* **2001**, 1769.

liquid-crystalline phenanthroline.[29] This is surprising because the flat and planar structure of phenanthroline should be highly suitable for assembling such frameworks via π stacking interactions into ordered mesophases. No results involving phenanthroline gels were disclosed, whereas terpyridine-containing carboxylic acid hydrogels have been described.[30] Furthermore, the straightforward coordination of metal centers could lead to the formation of novel metallomesogens displaying useful optical and/or electrical properties.[31]

We now describe phenanthroline ligands bearing a 1,3-diacylaminobenzene platform, which offers a suitable route for the inclusion of transition metals. The presence of a methyl group bisecting the central phenyl cycle is motivated by the need to tilt the amide vectors out-of-the-plane to favor intermolecular hydrogen bonding in the metal free ligand. From a general point of view, acylamino platforms have previously been selected as efficient gelators of various organic solvents.[32,33] Some of these gels appeared to have great potential as functional soft materials.[34,35] Recently, the gelation of room-temperature nematic liquid crystals by self-aggregation of low molecular weight molecules through hydrogen bonding has been reported, and this new class of liquid-crystalline materials have great potential in dynamic materials such as in electrooptic devices and as systems responsive to fast stimuli.[36,37] Furthermore, hexasubstituted phenyl rings with amide and alkynyl functions grafted with paraffin chains appear to be very interesting for the generation of one-dimensional nanostructures and surface-bonded lock-and-key receptors.[38]

Results and Discussion

Synthesis. The synthetic pathway for all compounds is sketched in Scheme 1. The starting materials 4-methyl-3,5-diaminobenzoic acid[39] and 2-hydroxy-9-methyl-1,10-phenanthroline[40] were prepared according to literature procedure. The key esterification step required the cross coupling between the acids (1^n) and the hydroxymethyl phenanthroline derivative with the chloride salt of 1-ethyl-3-[3-(dimethylamino)propyle]carbodiimide (EDC·HCl) in the presence of dimethylaminopyridine (DMAP). The use of dicyclocarbodiimide (DCC) was prohibited due to residual impurities always present in the final compounds.

The copper(I) complex was prepared under anaerobic conditions from ligands and [Cu(CH$_3$CN)$_4$]BF$_4$.[41] For ligand L[1], both BF$_4^-$ and ClO$_4^-$ counteranions were used. The last choice was motivated for single crystal growing. All organic compounds were purified by careful chromatography on silica, followed by double crystallization in adequate solvents. The air-stable copper complexes required two crystallizations to recover the analytically pure sample.

Characterization. The ^{1}H NMR spectra of the copper(I) complexes show major differences as compared to that of the free ligand (Figure 1). The most spectacular shifts are found for the phenyl protons H$_c$ (for labeling, see the drawing of the copper complex in Scheme 1), which are shielded by ca. 0.8 ppm, and for the methylene protons, which are shielded by ca. 1 ppm due to their proximity with the neighboring phenanthroline ring of the second ligand. This latter signal changes from a singlet in the free ligand to an AB quartet (with $J_{AB} = 10$ Hz and $\Delta\nu = 24$ Hz). The prochirality of these methylene protons is consistent with rigidification of the phenanthroline arms upon metal coordination. Finally, a significant upfield shift of the amides protons is observed from 8.23 ppm for ligand L[12] to 8.54 ppm for the complex. Similar shifts are found with complexes of ligands L[8] and L[16].

Upon diluting a sample of [Cu(L[1])$_2$]$^+$ from 5 to 0.05 mM, the single NH signal exhibits a very weak shift (<0.01 ppm), confirming the existence of intramolecular H-bonds.[42,43] Additional evidence for the prevalence of intramolecular H-bonds is provided by variable-temperature ^{1}H NMR studies from -10 to 50 °C in CDCl$_3$ which show progressive upfield shifts of -1.8×10^{-3} ppm K^{-1}. A similar trend of upfield shift was observed for the other copper complexes with weaker values (around -1.0×10^{-3} ppm K^{-1} with L[8], L[12], L[16]). Such effects were not observed in the metal-free ligands, excluding the presence of H-bonding at millimolar concentration in CDCl$_3$.

Infrared spectroscopy in solution and in the solid state for the copper complexes supports the claim that strong intramolecular H-bonding is occurring, whereas for the ligands only intermolecular interactions are effective. For the copper complexes, the ν_{NH} and ν_{CO} stretching vibrations were found, respectively, between 3230–3290 cm^{-1} and 1650–1660 cm^{-1} in the solid state. Very little changes were found in dilute CH$_2$Cl$_2$ solution (5 mmol), highlighting the occurrence of H-bonds in both states.[44] For the four ligands, the ν_{NH} and ν_{CO} stretching vibrations were found, respectively, between 3240–3260 cm^{-1} and 1645–1655 cm^{-1} in the solid state. In contrast, these ν_{NH} and ν_{CO} stretching vibrations were found at 3426 and 1677 cm^{-1} for L[12] and L[16] in dilute CHCl$_3$ solutions (ca. 1 mmol). This set of values is in the expected range for NH and C=O bonds involved in hydrogen bonds (for the complexes in solution and in the solid state and for the ligands only in the solid state), whereas for the ligands in solution the NH and C=O bonds are not involved in any supramolecular H-bonds as confirmed by the free NH and C=O stretching vibrations found at higher wavenumbers.[44]

Molecular Structures of the Ligand L[1] and the Corresponding [Cu(L[1])$_2$]ClO$_4$ Complex by X-ray Diffraction on

(29) (a) Date, R. W.; Iglesias, E. F.; Rowe, K. E.; Elliott, J. M.; Bruce, D. W. *Dalton Trans.* **2003**, 1914. (b) Camerel, F.; Strauch, P.; Antonietti, M.; Faul, C. F. J. *Chem.-Eur. J.* **2003**, *9*, 3764.
(30) Hanabusa, K.; Hirita, T.; Inoue, D.; Kimura, M.; Shirai, H. *Colloids Surf., A* **2000**, *169*, 307.
(31) (a) Serrano, J. L. *Metallomesogens*; VCH: Weinheim, 1996. (b) Serrano, J. L. *Prog. Polym. Sci.* **1997**, *21*, 873. (c) Stebani, U.; Lattermann, G.; Wittenberg, M.; Wendorff, J. H. *Angew. Chem., Int. Ed. Engl.* **1996**, *35*, 185. (d) Tschierske, C. *J. Mater. Chem.* **1998**, *8*, 1485. (e) Guillon, D. *Struct. Bonding* **1999**, *95*, 41.
(32) Hanabusa, K.; Yamada, M.; Kimura, M.; Shirai, H. *Angew. Chem., Int. Ed. Engl.* **1996**, *35*, 1949.
(33) Yasuda, Y.; Takebe, Y.; Fukumoto, M.; Inada, H.; Shirota, Y. *Adv. Mater.* **1996**, *8*, 740.
(34) Gu, W.; Lu, L.; Chapman, G. B.; Weiss, R. G. *Chem. Commun.* **1997**, 543.
(35) Hafkamp, R. J. H.; Kokke, B. P. A.; Danke, I. M.; Geursts, H. P M.; Rowan, A. E.; Feiters, M. C.; Nolte, R. J. M. *Chem. Commun.* **1997**, 545.
(36) Hikmet, R. A. M. *Mol. Cryst. Liq. Cryst.* **1991**, *198*, 357.
(37) Kelly, S. M. *J. Mater. Chem.* **1995**, *5*, 2047.
(38) (a) Nguyen, T.-Q.; Martel, R.; Avouris, P.; Bushey, M. L.; Brus, L.; Nuckolls, C. *J. Am. Chem. Soc.* **2004**, *126*, 5234. (b) Tuleski, G. S.; Bushey, M. L.; Kosky, J. L.; Ruter, S. J. T.; Nuckolls, C. *Angew. Chem., Int. Ed.* **2004**, *43*, 1836.
(39) (a) Pucci, D.; Weber, M.; Malthête, J. *Liq. Cryst.* **1996**, *21*, 153. (b) Pickaert, G.; Douce, L.; Ziessel, R.; Guillon, D. *Chem. Commun.* **2000**, 1584.
(40) Newkome, G. R.; Theriot, K. J.; Gupta, V. K.; Fronczek, F. R.; Baker, G. R. *J. Org. Chem.* **1989**, *54*, 1766.
(41) Hathaway, B. J.; Holah, D. G.; Poslethwaite, J. D. *J. Chem. Soc.* **1961**, 3215.
(42) Gong, B.; Yan, Y.; Zeng, H. Q.; Skrzypczak-Jankunn, E.; Kim, Y. W.; Hu, J.; Ickes, H. A. *J. Am. Chem. Soc.* **1999**, *121*, 5607.
(43) Gong, B. *Chem.-Eur. J.* **2001**, *7*, 4336.
(44) Hassner, A.; Alexanian, V. *Tetrahedron Lett.* **1978**, *46*, 4478.

Scheme 1*a*
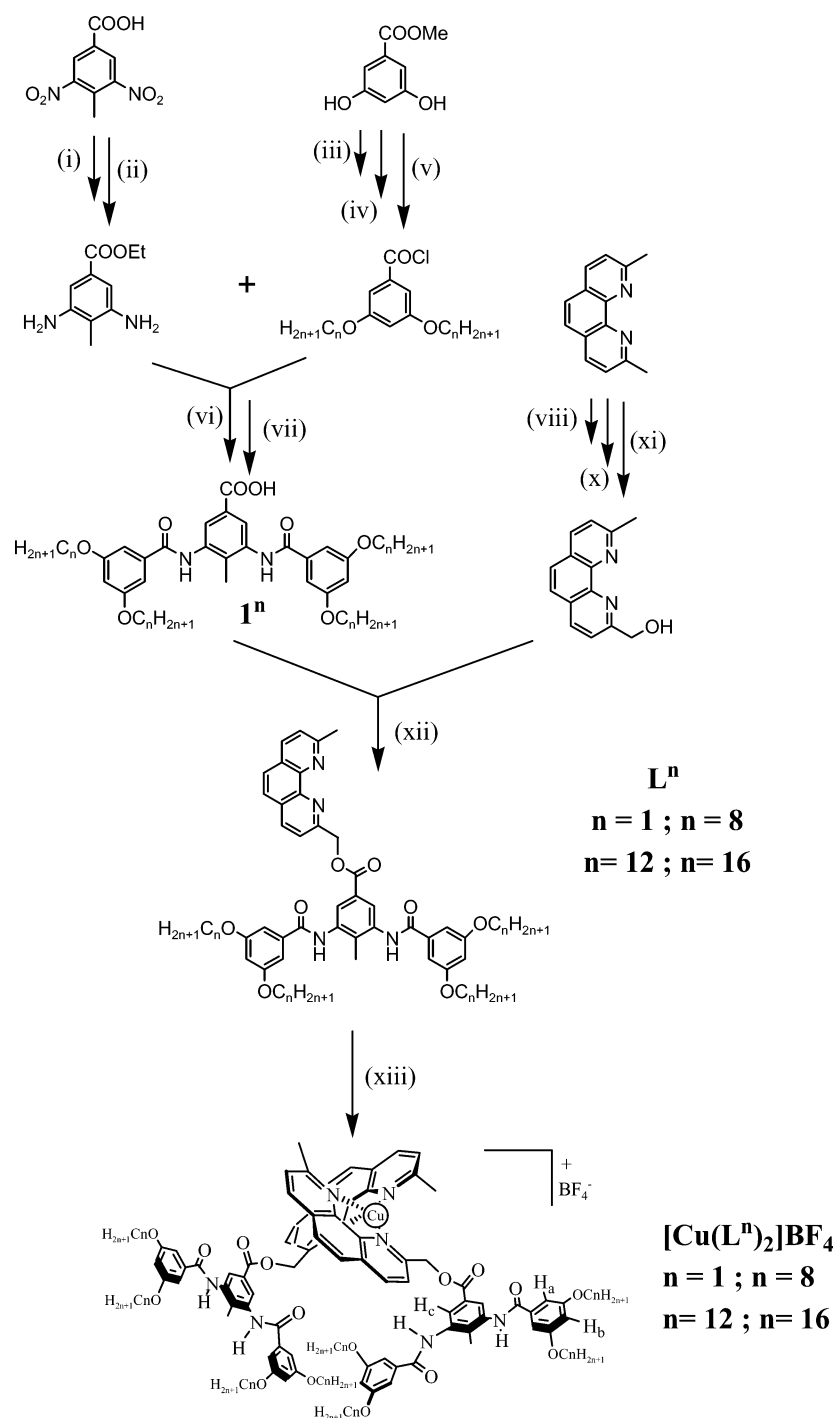
a Reagents and conditions: (i) EtOH reflux, H$_2$SO$_4$ (cat.), 89%; (ii) H$_2$, Pd/C (10 wt %), room temperature, EtOH/CH$_2$Cl$_2$, 99%; (iii) 1-bromoalkane, K$_2$CO$_3$, CH$_3$CN, reflux, 90% $n = 8$, 95% $n = 12$, 99% $n = 16$; (iv) EtOH, KOH, reflux, HCl (10%), 98% $n = 8$, 94% $n = 12$, 92% $n = 16$; (v) neat SOCl$_2$, reflux, quantitative; (vi) anhydrous Na$_2$CO$_3$, acetone, reflux, 75% $n = 1$, 72% $n = 8$, 78% $n = 12$, 78% $n = 16$; (vii) NaOH (50 equiv), THF/H$_2$O (v/v), reflux, 80% $n = 1$, 74% $n = 8$, 72% $n = 12$, 78% $n = 16$; (viii) *m*-CPBA, CH$_2$Cl$_2$, room temperature, 85%; (x) Ac$_2$O, reflux, 87%; (xi) K$_2$CO$_3$, EtOH, 50 °C, 92%; (xii) EDC·HCl (2 equiv), DMAP (1 equiv), CH$_2$Cl$_2$/THF, room temperature, 57% $n = 1$, 73% $n = 8$, 76% $n = 12$, 75% $n = 16$; (xiii) [Cu(CH$_3$CN)$_4$]BF$_4$, CH$_2$Cl$_2$, room temperature, 81% $n = 1$, 99% $n = 8$, 68% $n = 12$, 95% $n = 16$.

Single Crystals. Ligand L^1. The unique coordination features of the bis-amide framework were confirmed by a crystallographic structural determination of the parent compound in which the dialkoxy termini are replaced with methoxy groups. As expected, ligand L^1 is nonplanar; the peripheral trisubstituted rings are almost perpendicular with the central phenyl ring, while the phen subunit is tilted by 68° with respect to the central core

(Figure 2a). It is notable that the two amides vectors point in the opposite direction, which is auspicious for the formation of a polymeric network. Two remarkable features are evident from the packing of this compound. First, the central core of the crystal results from trimerization of the ligand via intermolecular hydrogen bonds, leading to the supramolecular edifice (Figure 2b). The tight hydrogen bonds connect, in a centrosymmetric
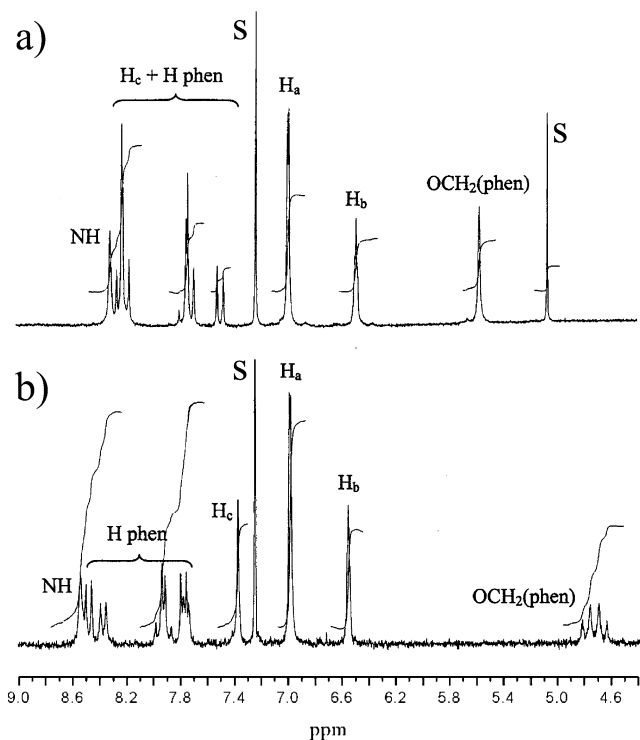
Figure 1. Proton NMR spectra of ligand L^{12} (a) and $[Cu(L^{12})_2]BF_4$ (b) recorded in CDCl$_3$ at 200 MHz and 298 K. For the sake of clarity, the CH$_2$ and CH$_3$ paraffin protons are not shown. S accounts for residual CHCl$_3$ and CH$_2$Cl$_2$ solvents.

fashion, the amide groups of the sandwich molecule I to the top molecule I′ (NH···O = 3.012(3) Å) and to the bottom molecule I″ (NH···O = 2.889(3) Å). The aromatic cores are loosely packed in a zigzag manner by weaker interactions (phenyl centroïd I/I′ = 4.4 Å and I/I″ = 3.7 Å).

Another interesting feature of the molecular structure is the π−π stacking of the phen fragments which runs along the diagonal of the β angle of the cell (standard distances lie in the range 3.5−3.6 Å, Figure S1). This strong stabilizing effect forces the welded hydrogen-bonded core to swing out of the stacks. As a consequence, one benzamide unit (Ar4) becomes involved in its own π−π stacking (d = 3.51 Å), while the Ar3 ring is essentially free of such interactions. Obviously, this infinite network is maintained by intermolecular hydrogen bonding, as well as by π−π stacking of the phen subunits.

Copper Complex [Cu(L¹)₂]ClO₄. As suggested by the ORTEP views of Figure 3, two L¹ ligands are interlocked around a single copper(I) atom in a pseudo-tetrahedral arrangement as usually found with this type of complexes.[45] The bite angles are 83.1(3)° and 82.0(3)°, respectively, for N(1B)−Cu−N(12B) and N(1A)−Cu−N(12A). For the sake of clarity and to describe the molecular structure and the crystal packing, we need to apply for ligand A the following: phenA, φ2A, φ3A, and φ4A will be, respectively, the phenanthroline subunit, the central aromatic core, and the two peripheral aromatic rings. For the second ligand B, we used phenB, φ2B, φ3B, and φ4B.

As compared with the free ligand, we can first notice a strong intramolecular hydrogen bond ($d_{N−O}$ = 3.015 Å) between two amide functions of the two interlocked ligands. Furthermore, additional hydrogen bonds are found between the N-atom (N$_a$)

(45) Juris, A.; Ziessel, R. *Inorg. Chim. Acta* **1994**, *225*, 251.
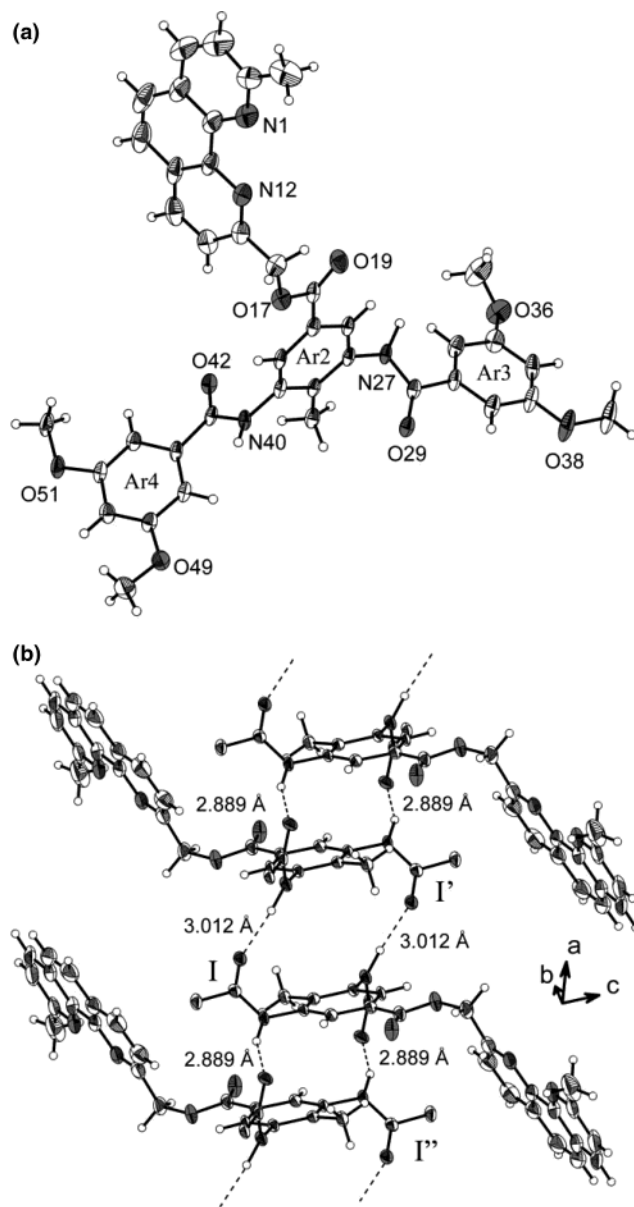

Figure 2. (a) Molecular structure of L¹ showing the atom-labeling scheme. The hydrogen-bonding schemes involving the amide groups are plotted as dotted lines. Angles between Ar2 and Ar3 = 82°; Ar2 and Ar4 = 84°. (b) Central trimeric core, setting up the building block of the supramolecular edifice. A single molecule I of L¹ [symmetry (x,y,z)] is surrounded by two others [symmetry (−x,−y,1 − z)] for I′ and [symmetry (1 − x,−y,1 − z] for I″. The hydrogen bonds (dotted lines) connect centrosymmetrically the amide groups of I to I′ (NH···O = 3.012(3) Å, NHO angle 173(1)°), and I to I″ (NH···O = 2.889(3) Å, NHO angle = 156(1)°). For the sake of clarity, the dimethoxyphenyl groups have been removed.

of one of those amide functions and the N-atom (N$_s$) of a solvent molecule ($d_{Na−Ns}$ = 3.082 Å). The two other amide functions interact with the N-atom of the acetonitrile molecule ($d_{Na−Ns}$ = 2.949 Å) and the perchlorate counteranion ($d_{Na−O}$ = 2.990 Å). In contrast with the free ligand, we noticed the lack of intermolecular hydrogen bonds between two neighboring complexes.

Concerning the two chelating subunits, we can first notice that phenA and phenB around a single copper are almost perpendicular with a dihedral angle of 89.96°. These fragments are almost parallel to the respective central phenyl ring with tilt angles of 7.95° between phenA and φ2B and of 7.87°
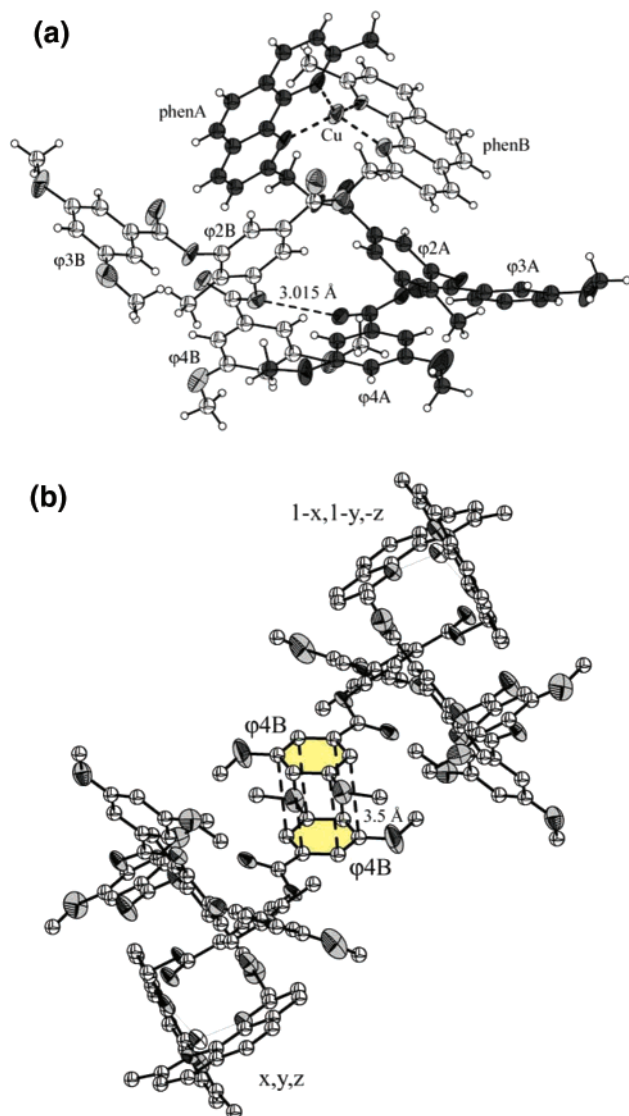
(a)

(b)

Figure 3. (a) ORTEP view of the molecular structure of the [Cu(L^1)$_2$]BF$_4$ complex; one of the interlocked ligands is colorized in black for the sake of clarity. (b) $\pi-\pi$ packing between two neighboring units.

Figure 4. Gelation test in cyclohexane: (a) L^{16} (5 g L^{-1}), (b) L^{12} (5 g L^{-1}), (c) [Cu(L^{16})$_2$]BF$_4$ (30 g L^{-1}). Gel formation is confirmed if the sample does not flow when the test tube is inverted (white arrows).

between phenB and φ2A. There is no intramolecular $\pi-\pi$ stacking, but we can observe a significant intermolecular $\pi-\pi$ interaction at a distance of 3.8 Å between phenA of one complex and φ3A of an adjacent complex. Furthermore, a second very strong $\pi-\pi$ stacking (at a centroïd–centroïd distance of 3.5 Å) involves two adjacent φ4B fragments belonging to two different complexes (Figure 3b).

Gelation Properties into Fibrous Aggregates. In light of the one-dimensional alignment of the amide-based phenanthroline ligands in the crystal structure supported by hydrogen-bonding interactions and $\pi-\pi$ interactions and the fact that the related copper complexes do not exhibit significant intermolecular interactions, it was tempting to involve such compounds in the formation of organogels and to observe the resulting behavior. The presence of the paraffin chains, in ligands L^{12} and L^{16}, features additional van der Waals interactions, useful in stabilizing the three-dimensional edifice. The gelation ability was evaluated in various polar or nonpolar, protic or nonprotic solvents (see Table S5). Both ligands displayed gelation abilities in cyclohexane and with linear alkanes from
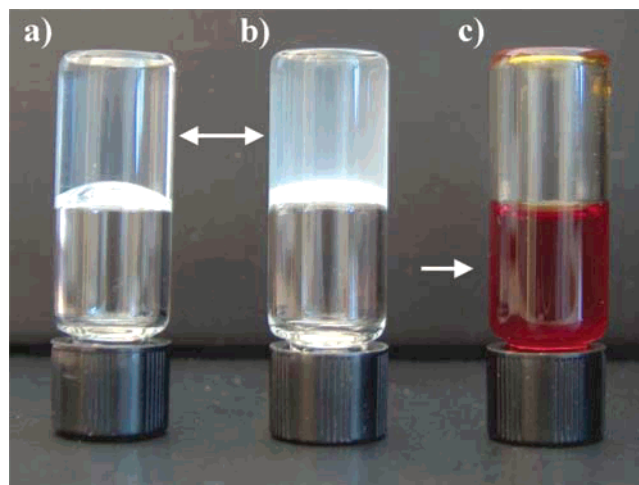
C$_6$ to C$_{12}$. Transparent gels were formed in cyclohexane and turbid gels were formed in hexane and dodecane at 25 °C, after heating a mixture of the ligand and the solvent to form a homogeneous fluid solution. Upon cooling below the temperature of gelation, the complete volume of solvent is immobilized and can support its own weight without collapsing as shown in Figure 4. The organogels exhibited thermally reversible sol-to-gel phase transitions. The minimum gelation concentrations (MGC) observed showed that these mesogenic ligands displayed good gelation abilities comparable with the ones already reported for other low molecular weight organogelators (see Table S5).[11c,46] Notice that ligand L^8, at a concentration of 6 g L^{-1}, does not give a gel in cyclohexane due to its lower solubility and its strong tendency to precipitate under these conditions. The unfavorable balance between the rigid part and the more flexible parts of the L^8 molecule avoids gelation.

SEM experiments were used to examine the morphology of these materials. Images obtained from a solution of L^{12} ligand in hexane (15.0 g L^{-1}) and L^{16} ligand in cyclohexane (16.5 g L^{-1}) dried onto silicon wafer reveals the presence of a 3D network of interlocked fibers with a diameter of ~140 nm extending over several micrometers (Figure 5a). It is likely that the formation of a 3D network of interlocked fiberlike aggregates is responsible for the immobilization, that is, the gelation, of hexane, cyclohexane, and dodecane. The width of the fibers is large compare to the dimension of the molecule. Therefore, the observed fibers correspond to a bundle of smaller elongated molecular assemblies (Figure 5b). The formation of elongated fiberlike aggregates indicates that the self-assembly of ligand L^{12} and L^{16} is driven by strong directional intermolecular interactions. To ascertain whether H-bonding plays a role in the formation of the observed fibers, infrared spectroscopy was performed in these gels. A single C=O stretching band was observed for L^{12} and L^{16}, respectively, at 1642 and 1645 cm^{-1}, in the three gelated solvents. Furthermore, a single NH stretching vibration at 3218 cm^{-1} in hexane, 3222 cm^{-1} in cyclohexane, and 3208 cm^{-1} in dodecane was observed for both ligands (as

(46) (a) Yasuda, Y.; Lishi, E.; Inada, H.; Shirota, Y. *Chem. Lett.* **1996**, 575. (b) Hanabusa, K.; Koto, C.; Kimura, M.; Shirai, H.; Kakehi, A. *Chem. Lett.* **1997**, 429. (c) Kimura, M.; Kobayashi, S.; Kuroda, T.; Hanabusa, K.; Shirai, H. *Adv. Mater.* **2004**, *16*, 335.
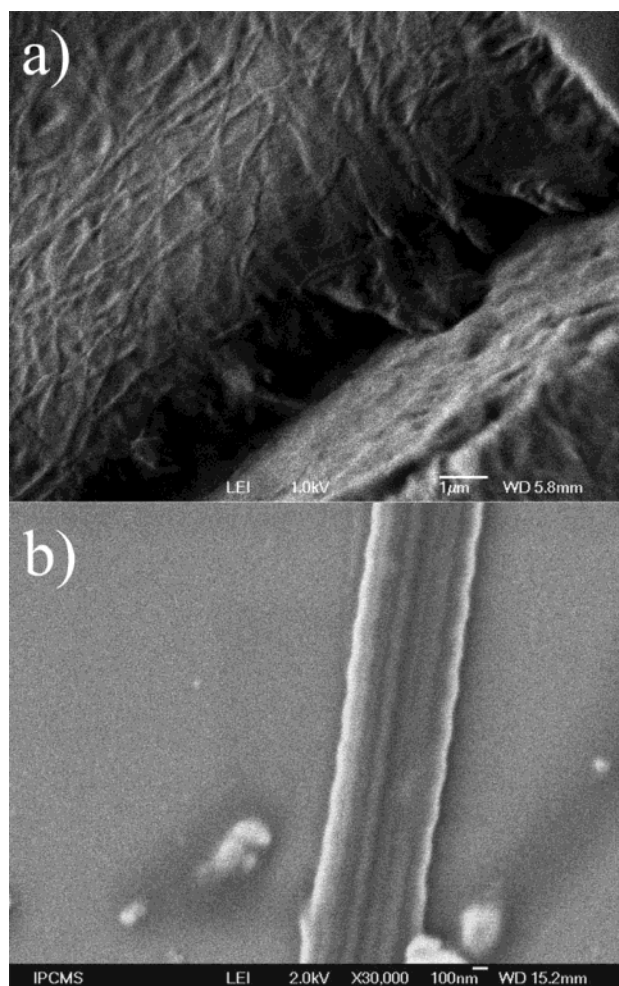
Figure 5. (a) SEM picture of a dried gel from ligand L^{16} in cyclohexane (16.5 g L^{-1}) deposited on silicon wafer showing the presence of fiber with an average diameter of ∼140 nm extended over several micrometers. (b) SEM picture of a freeze gel from a solution of L^{12} in cyclohexane (4.0 g L^{-1}) deposited on silicon wafer.

compared to 3426 cm^{-1} for the ligand in millimolar solution in CHCl$_3$). These spectroscopic data are an unambiguous signature of hydrogen-bonded amides inducing a hydrogen-bonded network, in line with the aggregation of the ligands into elongated fibers. It is also surmised that the $\pi-\pi$ interaction of the phenanthroline and/or phenyl subunits might add additional stabilization interactions.

The gelation ability of the copper(I) complexes with ligands L^{12} and L^{16} and BF$_4^-$ as counterion has also been investigated in cyclohexane, hexane, and dodecane. These complexes are soluble after heating but did not show any hint of gelation abilities at 25 °C even at a concentration as high as 40 g L^{-1}. With respect to the FT-IR data measured in these solvents and the previous discussion on these copper(I) complexes, it appears that because two amide groups are strongly engaged in an intramolecular hydrogen bond and the remaining amide functions are not suitably oriented to form an intermolecular network of hydrogen bonds, this would not lead to the gelation of the solvent. It is worth pointing out that the presence of charge is not inhibitory for the emergence of fiberlike aggregate.[13,47] These results confirmed that the switching of the hydrogen bonds from inter to intra when the ligands are interlocked around a metal

plays a crucial role in the gel formation but is not mandatory for the emergence of mesophase (vide infra).

Characterization and Mesomorphic Behavior of the Ligands and the Corresponding Complexes. The thermotropic properties of both ligands L^n and complexes [Cu(L^n)$_2$][BF$_4$] (n = 8, 12, 16) were investigated by a combination of differential scanning calorimetry (DSC), polarizing optical microscopy (POM), and small-angle X-ray diffraction studies (XRD).

The Ligands. Their polymorphic behavior was investigated systematically as a function of increasing and decreasing temperature on different batches of L^{12} and L^{16}. It appeared that the mesomorphic behavior strongly depends on the thermal history of the compound and upon kinetics that is presumably in keeping with the dynamics of hydrogen-bonding networks. L^8 was found to be deprived of mesomorphism over the tested temperature range (mp = 156 °C).

Observations by POM were rather laborious and confirmed the complicated thermal behavior of ligands L^{12} and L^{16}. On heating L^{12} above 90 °C, a cubic phase can be identified by X-ray diffraction through a diffraction pattern exhibiting two sharp reflections with the reciprocal spacing ratio $\sqrt{1}$ and $\sqrt{2}$ corresponding to a 3D cubic phase (at 23.3 and 16.2 Å, respectively, Figure S2) in the small region, and three broad halos at 7.5, 4.5, and 3.5 Å in the wide-angle region. Above 112 °C, another phase is growing alongside the cubic phase, and at 140 °C, the X-ray pattern is in agreement with the presence of a mixture of an isotropic liquid and small floating crystallites as proved by the presence of several sharp peaks in the medium and wide-angle regions. On further cooling and heating cycles, this high-temperature crystalline phase remains stable down to room temperature. Thus, the cubic phases seem to be only transient.

At room temperature, the X-ray pattern of ligand L^{16} is characteristic of a disordered lamellar crystalline phase. Above 110 °C, the X-ray pattern exhibits three sharp reflections (at 25.8, 17.6, and 14.9 Å) in the small-angle region and three broad halos at 7.5, 4.5, and 3.5 Å in the wide-range region (Figure S3). The three sharp reflections in the ratio 1, $\sqrt{2}$, and $\sqrt{3}$ suggest also a cubic phase. At higher temperature, above 115 °C, another mesomorphic phase appears, for which no firm identification was possible. At 125 °C, the compound becomes isotropic. On cooling, the cubic phase reappears at 115 °C with the same structural distances as on heating without showing the other mesophase (transient). Further heating and cooling cycles showed only the presence of the cubic phase above 71 °C (Cr 71 Cub 115 I). To confirm the thermal stability of the compounds, NMR spectroscopy was performed on samples kept 2 h at 125 °C (isotropic melt) and shows no sign of degradation. Furthermore, thermogravimetric analysis shows no weight loss up to 250 °C.

The Copper Complexes. Optical microscopy was not efficient in probing mesophase formation in these compounds, due to the absence of recognizable defects in the optical textures and to the high viscosity of the mesophases. However, on the basis of the molecular structure of the precursory ligands (vide supra), and the clipping effect induced by the copper cation and our previous experience with copper metallomesogens,[23,24]

(47) (a) Nakashima, T.; Kimizuka, N. *Adv. Mater.* **2002**, *14*, 1113. (b) Kuroiwa, K.; Shibata, T.; Takada, A.; Nemoto, N.; Kimizuba, N. *J. Am. Chem. Soc.* **2004**, *126*, 2016.

Table 1. Phase Transition Data from DSC and Data Collected from Powder-XRD Diffraction Patterns for the Copper Complexes

	DSC[a] mesomorphic properties	XRD[b] d_{meas}/(Å)	hk	l	d_{calc}/(Å)	parameters at T^c
[Cu(L[8])$_2$]BF$_4$	Cr 161 (28) I					
	I 96 (−10) Cr					
[Cu(L[12])$_2$]BF$_4$	Cr 75 (67) Col$_o$ 172 (34) I	41.0	20	VS	41.0	$T = 150$ °C
	I 135 (−29) Col$_o$					
		26.7	1$\bar{1}$	VS	26.7	$a_o = 83.0$ Å
		24.4	11	VS	24.4	$b_o = 27.1$ Å
		20.1	40	M	20.5	$\gamma = 98.75$°
		9.0		br	h2	$S_o = 2225$ Å^2
		4.5		br	h1	
[Cu(L[16])$_2$]BF$_4$	Cr 62 (145) Col$_o$ 164 (24) I	42.1	20	VS	42.1	$T = 150$ °C
	I 132 (−22) Col$_o$					
		32.0	1$\bar{1}$	VS	32.0	$a_o = 85.5$ Å
		28.5	11	VS	28.5	$b_o = 32.7$ Å
		21.2	40	M	21.05	$\gamma = 99.95$°
		15.75	2$\bar{2}$	W	16.0	$S_o = 2755$ Å^2
		9.0		br	h2	
		4.5		br	h1	

[a] Transition temperatures (°C), and enthalpy of transitions (ΔH/kJ mol^{-1}); Cr, crystalline phases; I, isotropic liquid; Col$_o$, oblique columnar phase. [b] hk are the indexations of the reflections corresponding to the Col$_o$ phase, and I is the intensity of the reflections (VS, very strong; S, strong; M, medium; W, weak; br, broad); d_{meas} and d_{calc} are the measured and calculated diffraction spacing values. [c] a_o and b_o are the lattice parameters of the Col$_o$ phase ($a_o = \frac{2d_{20}}{\sin \gamma}$; $b_o = \frac{A}{\sin \gamma}$; $A = \sqrt{\dfrac{2}{\dfrac{1}{d_{11}^2} + \dfrac{1}{d_{1\bar{1}}^2} - \dfrac{1}{2d_{20}^2}}}$), γ is the angle between a_o and b_o, and S_o is the lattice area ($S_o = a_o b_o \sin \gamma$).

mesomorphic behavior was anticipated for the fully interlocked complex. During the first heating, several endothermic peaks could be observed on the DSC traces, suggesting at least a polymorphic behavior (Table 1). However, on subsequent heat–cool cycles, the DSC traces appeared simpler. From the large enthalpy value measured at high temperature, corresponding to the transition to the isotropic state (POM), again, the octyloxy derivative did not appear to be mesomorphic. In contrast, the dodecyloxy and hexadecyloxy derivatives likely exhibited mesomorphism, as much smaller enthalpies were measured at the clearing transitions (Table 1).

To identify the mesophases, variable-temperature powder-XRD experiments were carried out from the crystalline state up to the isotropic liquid. The transition temperatures detected by DSC and optical microscopy were in good agreement with those derived from XRD. The crystalline phases displayed a series of sharp peaks over the entire range of 2θ. The transformation to the mesophase was accompanied by the disappearance of a number of these sharp reflections and significant changes in intensity in others. The X-ray diffraction patterns supported the presence of liquid-crystalline mesophases for the two long-chain complexes (Figure 6) and confirmed the absence of any mesophase for the octyloxy complex.

The X-ray patterns for the two complexes are similar (Figure 6) and divided into three different regions as follows:

(i) At wide angles, a diffuse and broad-scattering halo was observed centered around 4.5–4.6 Å (h1), corresponding to the liquidlike order (short-range correlations) of the molten chains bound to the complexes, and thus to the fluidlike nature of the mesophase.

(ii) At slightly lower angles, another weak, less diffuse halo, was seen, associated to a distance of ca. 9.0 Å (h2) which was attributed to some liquidlike correlations between neighboring molecules. This broad scattering suggests a loose periodicity of the molecular species inside the columns, although this was not correlated over too great a distance.
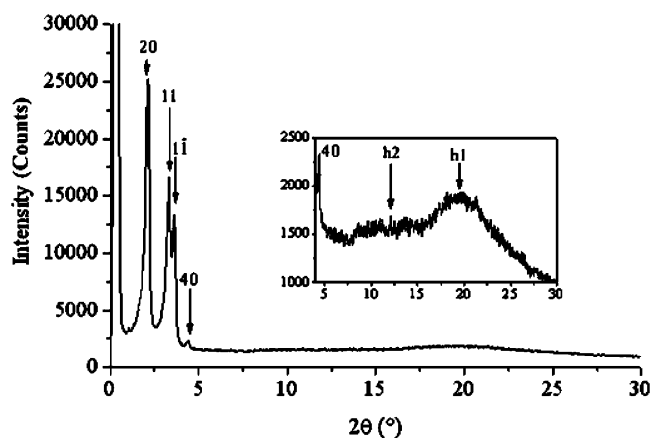
Figure 6. XRD diffraction patterns of the complex [Cu(L[12])$_2$]BF$_4$ recorded at 423 K.

(iii) Finally, in the small-angle region, a series of several Bragg peaks were present. Three sharp and intense reflections of more or less equal relative intensity were observed which could be indexed with the fundamental (20), (11), and (1$\bar{1}$) reflections corresponding to a 2D oblique lattice.[48,49] One or two more higher order reflections of smaller intensity could also be observed and were indexed as (40) for $n = 12$, and (40) and (2$\bar{2}$) for $n = 16$. The sharpness and intensity of the small-angle reflections also indicate the long-range correlation of the 2D arrangement of the columns (Col$_o$ phase).

Therefore, the effect of the complexation of a metallic center with this organic platform results in a dramatic change of the mesomorphic properties. First, the mesophase stability has been greatly enhanced upon the coordination to copper(I), particularly due to the huge increase of the clearing temperature, the melting temperature remaining almost the same for the ligands and

(48) Levelut, A. M. *J. Chim. Phys.* **1983**, *80*, 149.
(49) Morale, F.; Date, R. W.; Guillon, D.; Bruce, D. W.; Finn, R. L.; Wilson, C.; Blake, A. J.; Schröder, M.; Donnio, B. *Chem.-Eur. J.* **2003**, *9*, 2484.
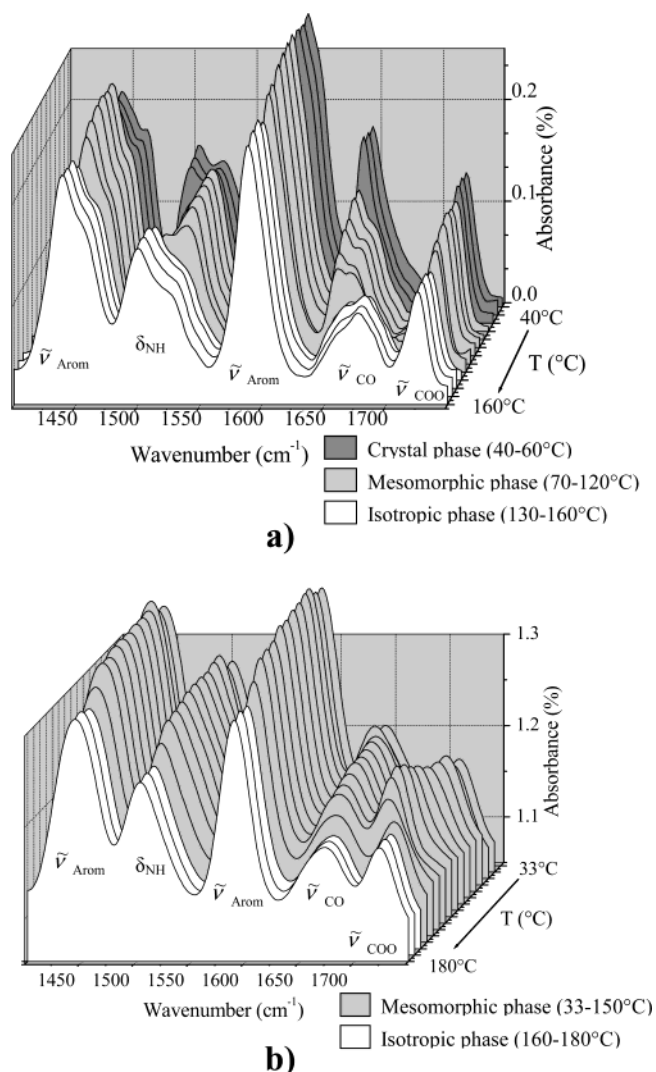
Figure 7. FT-IR spectra (from 1400 to 1750 cm^{-1}) recorded for compound L^{12} (a) and its [Cu(L^{12})$_2$]BF$_4$ complex (b) versus temperature in the range 40−160 °C for L^{12} and 33−180 °C for the copper complex. The measurements were carried out with polished KBr disks starting from the crystalline phase.

corresponding complexes. On average, the mesophase stability is increased by nearly 50 °C. The second important consequence was the thermodynamic stability of the Col$_o$ phase for the metal complexes when compared to the corresponding ligands.

Infrared in the Mesophases. Evidence for the persistence of hydrogen bonding in the mesophase was obtained by variable-temperature FT-IR spectra for the ligands and complexes dispersed onto KBr pellets. For both ligands, a weakening of ν_{N-H} stretching vibrations with shifts, from 3228 cm^{-1} in the crystalline phase to 3290 cm^{-1} in the isotropic phase, was observed. In the crystalline phase, the C=O stretching vibration appears as a single band at 1645 cm^{-1}, and, after melting in the mesomorphic phase, a new band appears at 1655 cm^{-1} with a concomitant and progressive decrease of the original band. Both bands are characteristic of H-bonded amides. Furthermore, in the isotropic phase (over 120 °C), this band is split and shifts to peaks at 1657 cm^{-1} (H-bonded amide) and 1673 cm^{-1} (free amide, Figure 7a). A similar behavior is found for the NH bending vibration. These latter values are in agreement with previous studies on mesogenic hydrogen-bonded amide ag-

gregates.[50] As expected, no weakening or shift of the C=C and COO bands could be seen during the heating process. The splitting of the C=O stretch and N−H bend peaks, and the quasi-disappearance of the original vibrations, during the heating process suggest that the formation of the mesomorphic state from the solid involves severe internal reorganization and the occurrence of at least two different types of hydrogen bonds involving the amide functions. It is likely that the presence of two hydrogen bonds in the mesophase is associated with a different packing of the phenanthroline cores upon microsegregation. In contrast, for the copper(I) complexes, the single intramolecular H-bond persists in the solid, mesomorphic, and isotropic states with no major perturbations of the energy and intensity of the ν_{CO}, ν_{NH}, and δ_{NH} stretching and deformation vibrations (Figure 7b). It is surmised that the two remaining NH−CO junctions are possibly involved in hydrogen bonds with the counteranions. Such additional intracomplex hydrogen bonds are present in the X-ray structure of the [Cu(L^1)$_2$]ClO$_4$ complex and would explain the fact that no free NH−CO vibrations were observed in the FT-IR spectra. Likewise, the switching of one hydrogen bond provides thermally stable complexes but avoids the emergence of an extended hydrogen-bonded network that is a prerequisite for gelation of solvents but is not damageable for the formation of mesophases. Switching the ester linkage into an amide linkage could add additional stabilization interactions.

Packing Study of the Copper(I) Complexes and Structure of the Col$_o$ Phase. To get some insight on the molecular packing within the columns and to have a better understanding of the 2D arrangement of the columns, a geometrical approach previously used[49] and based on the segregation of the chemically different constituting parts of the molecules (hard parts and aliphatic chains) has been applied. From such a point of view, columnar structures are mainly characterized by two geometrical parameters: the columnar cross section, S_{col}, and the stacking periodicity along the columnar axis, h,[51] which are mutually linked analytically through the relation $hS_{col} = NV_m = V_{cell}$, where N is the number of molecules within a columnar stratum and V_m is the molecular volume. Note that h is obtained directly from the X-ray patterns (vide supra) and corresponds to the stratum thickness, and the molecular volume, V_m, and the cross-sectional areas of the columns are derived from crystallographic and XRD data. Moreover, on the basis of the amphiphilic character of such materials,[49,52] it is also possible to express the molecular volume as the sum of elementary volumes using the additivity rule of the partial volumes according to $V_m = V_{Ar} + V_{CH}$, where V_{Ar} is the volume of the aromatic, polar part, and V_{CH} is the volume of the paraffin chains.[48] Knowing these volumes, and thus the associated volume fraction of the column occupied solely by the hard molecular parts, f_{Ar} ($=V_{Ar}/V_{mol}$), the cross section of the columnar inner core, S_{Ar}, can also be calculated according to $S_{Ar} = f_{Ar} \cdot S_{col}$. These general equations will be used in the following discussion.

(50) (a) Kato, T.; Kutsuna, T.; Hanabusa, K.; Ukon, M. *Adv. Mater.* **1998**, *10*, 606. Silverstein, R. M.; Bassler, G. C.; Morrill, T. C. *Spectrometric Identification of Organic Compounds*, 3rd ed.; Wiley: New York, 1976. (b) Hanabusa, K.; Kato, C.; Kimura, M.; Shirai, H.; Kakehi, A. *Chem. Lett.* **1997**, 429.
(51) Guillon, D. *Struct. Bonding* **1999**, *95*, 41.
(52) (a) Skoulios, A.; Guillon, D. *Mol. Cryst. Liq. Cryst.* **1988**, *165*, 317. (b) Tschierske, C. *J. Mater. Chem.* **1998**, *8*, 1485. (c) Tschierske, C. *J. Mater. Chem.* **2001**, *11*, 2647. (d) Tschierske, C. *Annu. Rep. Prog. Chem., Sect. C* **2001**, *97*, 191.
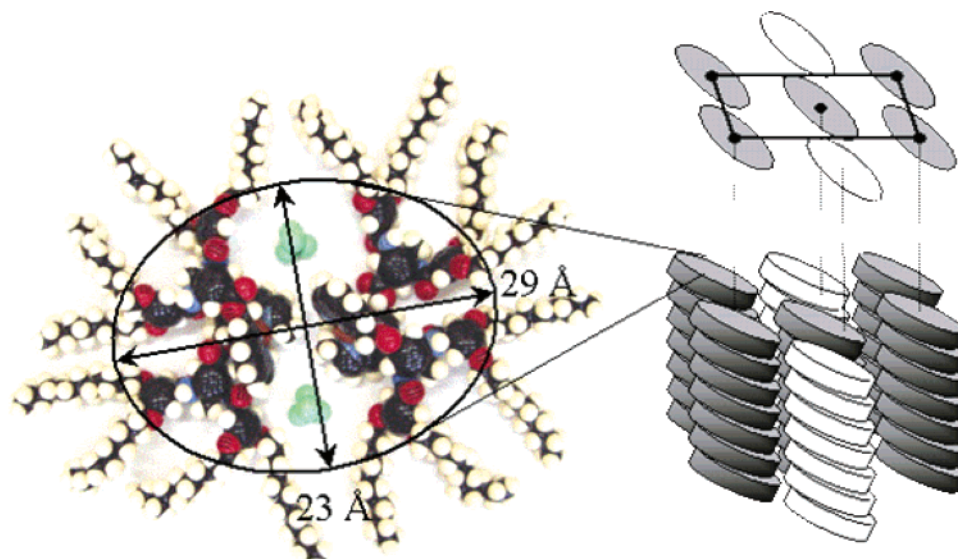
Figure 8. (a) CPK model of two molecules of [Cu(L^{12})$_2$]BF$_4$ complex (arbitrary number of carbons) forming an elliptical plateau and (b) schematic representation of this plateau within the columnar mesophase with an oblique symmetry and a tilt of ca. 40°. The adjacent BF$_4^-$ anion within the disk is located arbitrary to fill the empty space, thus improving molecular packing within the mesophase.

Table 2. Crystallographic Data of the Mesomorphic Complexes^a

	S_{col} (Å^2)	$V_{cell} = S_{col} \times h2$ (Å^3)	V_m (Å^3)	N
[Cu(L^{12})$_2$]BF$_4$	1112.5	10 020	5070	2.0
[Cu(L^{16})$_2$]BF$_4$	1377.5	12 400	5890	2.1

^{a} $S_{col} = S_o/2$. V_{cell} is the volume of one columnar stratum $h2$-thick. Molecular volume, $V_m = \dfrac{M}{0.6022} \dfrac{V_{CH_2}(T)}{V_{CH_2}(T_0)}$; M, molecular weight; $V_{CH_2}(T)$ = 26.5616 + 0.02023T; T in °C, $T_0 = 22$ °C; N, number of molecules per V_{cell}.

Finally, let us recall that, in columnar phases, the lattice plane is defined as the plane that is perpendicular to the columnar axis, and the 2D symmetry results from the shape (circular or elliptical), disposition, and mutual orientations (for ellipses only) of the columnar cross sections. In the Col$_o$ case, the columnar cross section is not circular as in the Col$_h$ phase, but adopts an elliptical shape, and the particular disposition of the elliptical columnar cross sections leads to an oblique lattice (Figure 8), with two columns per cell.[49] Note that the oblique lattice determined in this work does not differ much from a rectangular cell, the angle γ between the lattice parameters a_o and b_o being ca. 100°, thus corresponding to a slight distortion of the rectangular cell.

In the case of the complexes, V_m values were estimated considering a density of 1 in the mesophase, and were then corrected by a temperature factor because the volume increases with temperature (Table 2).[53–55] Such a value for the density is acceptable and is commonly used in liquid crystals. It was found

that the volume of one complex corresponds to exactly the volume of a columnar stratum having a thickness of 4.5 Å ($h1$). The thickness of the complex is, however, larger, in the range of 9–10 Å. It is therefore necessary to take into account the doubling of the periodicity, and thus to consider a columnar slice twice as thick of 9 Å, which in fact corresponds to the position of the second broad scattering observed in the XRD patterns (i.e., $h2 = 9$ Å). To propose a suitable organization of the complexes within the column, calculation of S_{Ar}, the cross section of the inner columnar core, seems to indicate that the two complexes lie roughly side-by-side within the columnar slice, with the two anions located in the voids created by such molecular disposition. This value is in the range with the dimensions of the dimeric arrangement as illustrated by the CPK model shown in Figure 8. Stricto sensu if the dimer adopts such a conformation, the area described by the ellipse should be reduced either by the tilt of the elliptical plane with respect to the columnar axis or by the shortening of the longer axis of the ellipse to compensate the calculated surface area of the inner columnar core. A value of ca. 400–420 Å^2 ($f_{Ar} = 35.9\%$ for $n = 12$, and 30.9% for $n = 16$) was actually found for the surface area of the inner core, smaller than the 525 Å^2 obtained from the CPK model ($S = \pi ab/4$, where $a = 29$, $b = 23$), implying a tilt of ca. 40° of the assembly with respect to the columnar axis. To keep the elliptical shape, the tilt must occur around the long molecular axis of the ellipse to satisfy the limits imposed by the oblique lattice to fix the columns as schematically depicted in Figure 8.

Conclusion

A central 4-methyl-3,5-diacylaminobenzene core equipped with an ester group connected to a phenanthroline subunit and two secondary amide functions each carrying a phenyl ring with two paraffin chains has been prepared by a rational approach and subsequently easily and quantitatively transformed into deep red and stable copper(I) complexes. The amide functions are clearly involved in a supramolecular hydrogen-bonded network, whereas one hydrogen bond is frustrated into a tight intra-

(53) The molecular volume of the ligand L^1 was obtained experimentally by crystallography ($V_m = 842.5$ Å^3). V_{CH} was calculated as follows (all elementary volumes in Å^3 and T in °C): $V_{ch} = 4 \times 12 \times V_{CH_2} + 4\Delta V_{CH_3}$, where $V_{CH_2} = 26.5616 + 0.02023T$ and $\Delta V_{CH_2} = 27.14 + 0.01713T + 0.0004181T^2$ represents the volume difference between the terminal methyl group and a methylene group. $V_{Ar} = 625$ Å^3 at 22 °C and 660 Å^3 at 90–95 °C.
(54) Molecular volume $V_m = (M/0.6022)(V_{CH_2}(T)/V_{CH_2}(T_0))$; M, molecular weight; $V_{CH_2}(T) = 26.5616 + 0.02023T$; T in °C, $T_0 = 22$ °C.
(55) The molecular volume of the complex [Cu(L^1)$_2$]ClO$_4$ obtained experimentally by crystallography was $V_m = 2095.5$ Å^3. $V_{Ar} = 1660$ Å^3 at 22 °C and 1820 Å^3 at 150 °C. Using the same method as in ref 53 would give 4900 and 5850 Å^3 for the volume of [Cu(L^{12})$_2$]ClO$_4$ and [Cu(L^{16})$_2$]ClO$_4$, respectively, at 150 °C, in good agreement.

molecular bond during the interlocking of two such ligands around a copper center. A remarkable feature of the free ligands ($n = 12$ and 16) is the gelation of hydrocarbon solvents. SEM measurements reveal that 3D dimensional networks are formed of interlocked fibers with a diameter of ~140 nm extending over several micrometers in length. This supramolecular organization is likely facilitated by a combination of three types of molecular interactions: hydrogen bonding, van der Waals interactions within the paraffin chains, and $\pi-\pi$ stacking interactions between the phenanthroline and/or the phenyl rings, ensuring an optimal immobilization of the solvents. Because of the emergence of a very strong intramolecular hydrogen bond, the copper complexes are not organogelators. Liquid-crystalline mesomorphism was found for the free ligands (transient for $n = 12$ and enantiotropic for $n = 16$), and heating the related copper complexes also affords mesomorphic materials packed in a columnar mesophase with an oblique 2D symmetry. Even if the starting molecular shape of the complex does not follow the strict criteria of structural anisometry, LC mesomorphism can be provided here through the interplay of specific interactions that favor the desired self-organization of the molecules. A careful study by FT-IR of the free ligands revealed the presence of strong H-bonds in the crystalline state, organogel, and liquid-crystalline phase but not in dilute solutions. However, in the copper(I) complexes, two ligands are sealed via a strong intramolecular hydrogen bond between the C=O bond of one ligand and the NH bond of the second ligand which persists even in polar solutions.

The present system describes unique examples of organogelators as well as a thermotropic phenanthroline-based metallomesogen. It is worth pointing out that, contrary to the previous cases where oligopyridines are involved in mesomorphic matter, the use of a potential hydrogen-bond director allows for the production of mesomorphic materials with both ligands and complexes. This work demonstrates guidelines for programming transition metal complexes into self-assembled nanostructures. The idea leading to the generation of these materials can be used to design novel functional complexes ordered in soft condensed matter with potential applications in nanoelectronics, light-emitting layers, and photovoltaics. Research along this line is currently in progress in our laboratory.

Supporting Information Available: Complete experimental section including the preparation and characterization of the ligands and complexes. Summary of crystal data, intensity measurements, and structure refinement for L^1 (Table S1) and for [Cu(L^1)$_2$]ClO$_4$ (Table S3), selected hydrogen bonds for ligand L^1 (Table S2), and the [Cu(L^1)$_2$]ClO$_4$ complex (Table S4). Schematic representation of the interdigitated phen subunits is given in Figure S1. Gelation tests and minimum gel concentration (g L^{-1}) (Table S5). XRD diffraction patterns of L^{12} recorded at 373 K and L^{16} recorded at 383 K are given in, respectively, Figures S2 and S3. CIF files for the X-ray structure determinations are also available. This material is available free of charge via the Internet at http://pubs.acs.org.

JA047091A